The Geological Orrery: Mapping Chaos in the Solar System

Paul E. Olsen[1], Jacques Laskar[2], Dennis V. Kent[3,1], Sean T. Kinney[1], David J. Reynolds[4], Jingeng Sha[5], and Jessica H. Whiteside[6]

[1]*Lamont-Doherty Earth Observatory of Columbia University, Palisades, NY 10968 U.S.A.*

[2]*Astronomie et Systèmes Dynamiques, IMCCE-CNRS UMR8028, Observatoire de Paris, UPMC, 77 Avenue Denfert-Rochereau, 75014 Paris, France.*

[3]*Earth and Planetary Sciences, Rutgers University, Piscataway, NJ 08854, U.S.A.*

[4]*ExxonMobil Exploration Company, Houston TX, U.S.A.*

[5]*State Key Laboratory of Palaeobiology and Stratigraphy, Nanjing Institute of Geology and Paleontology and Center for Excellence in Life and Paleoenvironment, Nanjing 210008, China .*

[6]*Ocean and Earth Science, National Oceanography Centre, University of Southampton, European Way, Southampton, SO14 3ZH U.K.*

Corresponding Author: Paul E. Olsen

ABSTRACT

The Geological Orrery is a network of geological records of orbitally-paced climate designed to address the inherent limitations of solutions for planetary orbits beyond 60 Ma due to the chaotic nature of Solar System motion. We use results from two scientific coring experiments in early Mesozoic continental strata: the Newark Basin Coring Project and the Colorado Plateau Coring Project. We precisely and accurately resolve the secular fundamental frequencies of precession of perihelion of the inner planets and Jupiter for the Late Triassic and Early Jurassic epochs (223 to 199 Ma) using the lacustrine record of orbital pacing tuned only to one frequency (1/405 ky) as a geological interferometer. Excepting Jupiter, these frequencies differ significantly from present values, as determined using three independent techniques yielding practically the same results. Estimates for the precession of perihelion of the inner planets are robust, reflecting a zircon U-Pb-based age model and internal checks based on the overdetermined origins of the geologically measured frequencies. Furthermore, while not indicative of a correct solution, one numerical solution closely matches the Geological Orrery with the probability due to chance being less than 5 x10^{-8}. To determine the secular fundamental frequencies of the precession of the nodes of the planets and the important secular resonances with the precession of perihelion, a contemporaneous high-latitude geological archive recording obliquity pacing of climate will be needed. These results form a proof-of-concept of the Geological Orrery and lay out an empirical framework to map the chaotic evolution of the Solar System.

Significance Statement

The Solar System is chaotic and precise solutions for the motions of the planets are limited to about 60 million years. Using a network of coring experiments we call the Geological Orrery, (after 18th century planetaria), we recover precise and accurate values for the precession of the perihelion of the inner planets from 223 to 199-million-year-old tropical lake sediments, circumventing the problem of Solar System chaos. Extension of the Geological Orrery from 60 million years ago to the whole Mesozoic and beyond would provide a new empirical realm to constrain models of Solar System evolution, further test General Relativity and its alternatives, constrain the existence of additional past planets, and test predictions of dark matter interactions with the Solar System.

In the introduction of his 1812 treatise on probability, Pierre-Simon de Laplace (1) envisioned the possibility of modeling the whole universe in a single equation (the gravitational laws). Using only knowledge of the present initial conditions, one could recover all the past and predict all the future. But this paradigm of determinism does not apply to the Solar System. The validity of the solutions of Solar System gravitational models is constrained to about 0-60 Ma not only because of inherent limitations in the determination of initial conditions and parameters of the model, but more fundamentally because of the chaotic nature of the system for which initially close solutions diverge exponentially, in fact multiplying the uncertainties by a factor of 10 every 10 My (2,3). Although there has been much recent progress, the powerful constraint imposed by chaos, at several levels, means that it is hopeless to attempt to retrace the precise history of the Solar System from only knowledge of the present, as has been done until now. Conversely, geological data can constrain the astronomical solution back in time, thus allowing us to go beyond the horizon of predictability of the system. Geological data recording climate variations modulated by celestial mechanics potentially provide an empirical realm to test astronomical solutions that must conform to the past. Geological data from within the last 60 My seem to agree with astronomical solutions (4,5) but provide little information on the Solar System beyond what is already known. The fundamental challenge is to find empirical data well beyond 60 Ma to provide anchors for extending the astronomical solutions, but this quest has been hampered by a lack of records with both sufficient temporal scope and independent age control. To circumvent the limitations of most geological data we have developed an experimental system that uses a plexus of highly resolved data from multiple temporally correlative and complementary records termed “The Geological Orrery”, named after the mechanical planetaria - Orreries - of the 18th century, from the 4th Earl of Orrery, Charles Boyle (6), and the “Digital Orrery”, a dedicated parallel-processing computer that was constructed to investigate the long term motion of the Solar System that numerically confirmed its chaotic nature (7,8). The Geological Orrery provides a procedure to fully map the actual gravitational history of the last ~250 My of the Solar System and beyond allowing reliable filtering and modification of astronomical solutions.

To a first approximation, the orbital planes of the planets are slowly deformed by the gravitational forces of the other bodies in the Solar System in a quasiperiodic way that can be decomposed into a series of secular fundamental frequencies representing roughly each planet’s contribution to the deformation of the orbits. These motions can be described in terms of the precession of perihelion in the orbital plane (with the g_i frequencies) and the precession of the orbital plane in space represented by the precession of the node (with the s_i frequencies). Difference frequencies of these secular frequencies of precession of perihelion g_i yield the “eccentricity cycles” familiar to paleoclimatologists, and the sums of the g_i frequencies with Earth’s axial precession constant, p, yield the “climatic precession” frequencies, today averaging about 21 ky (Table 1). Similarly, the difference frequencies of the secular fundamental frequencies of precession of the orbital nodes s_i yield the orbital inclination frequencies and the sums of the s_i frequencies with p yield the familiar obliquity periods today near 41 ky.

Here we use the Geological Orrery to precisely determine the secular fundamental frequencies of the precession of perihelion of the inner planets and Jupiter from 199-220 Ma using climate proxy and geochronologic results from two major

scientific coring experiments: 1) Newark Basin Coring Project (NBCP) (9) that form the basis of the Newark–Hartford Astrochronostratigraphic Polarity Timescale (N–H APTS) (10) along with new data from the adjacent Hartford Basin (see Appendix SI); and 2) the Colorado Plateau Coring Project (CPCP–1) (11,12) (Fig. 1, *SI Appendix* Fig. S6 and Table S1).

The NBCP experiment collected seven ~1000 m continuous cores and core holes in lacustrine to fluvial rift basin strata of the Newark Basin spanning most of the Late Triassic and the earliest Jurassic which together with additional core and outcrop data (13,14,15, *SI Appendix,* Figs. S1,S6; Table S1), tested the permeating nature of orbital pacing of lake depth in the paleotropics (0° - 21° N, ref. 16) through the lacustrine part of the section, previously inferred from scarce and discontinuous outcrops (17,18,19). Global correlation is achieved through sixty-six geomagnetic polarity intervals pinned in time by zircon CA-ID-TIMS U-Pb dates from three lava flow formations interbedded in the very latest Triassic and earliest Jurassic age part of the sequence (20,21). Using largely a facies classification and a color scale, the NBCP experiment (19) supported the hypothesis that the rift lake depth was paced by orbital cycles including a full range of climatic precession-related cycles. These include the ~20 ky precessional and the ~100, and 405-ky orbital eccentricity cycles with the latter, and its mappable geological equivalent termed the McLaughlin Cycle (Table 1), then being used to tune the entire lacustrine part of the composite Newark-Hartford record (22). This in turn, allowed the Triassic values of the secular fundamental frequencies of the precession of perihelion for Mercury (g_1), Venus (g_2), Earth (g_3), and Mars (g_4) (Table 1) to be roughly estimated (22). The tuned data also revealed even longer-period “Grand Cycles” (23) (Table 1), including one with a period of ~1.7 My identified as the Mars-Earth cycle (g_4-g_3), that today has a value of ~2.4 My (4); the difference being attributed to chaotic diffusion in the behavior of the Solar System. However, these results lacked independent age control allowing the possibility that hiatuses invisible to spectral analysis compromise both the timescale and the apparent eccentricity periodicities longer than 405 ky (24,25,26,27).

A major goal of the CPCP–1 experiment in the Triassic Chinle Formation in Petrified Forest National Park in Arizona was to provide an independent zircon U-Pb age-constrained paleomagnetic polarity stratigraphy that could be correlated to and test the NH APTS and the application of orbital theory on which it is based (11). CPCP–1 validated the NH APTS interval from ~210 to 215 Ma and implicitly validated the age model for the younger interval bounded by zircon CA-ID-TIMS U-Pb dates from Newark Basin lavas for ~600 ky around ~201 Ma (21) making an independently dated sequence extending from ~201 to 215 Ma in total. These geochronological data validate the NH APTS, and provide direct dating of the 405 ky cycle 215 million years ago (12) (*SI Appendix* Fig. S7; Table S2), and provide the needed age control for examining Triassic-Early Jurassic orbital frequencies in the Newark-Hartford data set and permit direct comparison to Neogene and Quaternary marine data.

Newark-Hartford composite results

The newly compiled Newark-Hartford data set consists of four major depth series: depth rank (sedimentary facies related to water depth) and color from the

recovered cores, and down-hole sonic velocity and natural gamma radiation measurements providing instrumental complementary data (*SI Appendix,* Figs. S2,S6) New data from cores and outcrops from the Newark and Hartford basins allow seamless extension of the sequence into the Early Jurassic (Hettangian and early Sinemurian) (*SI Appendix* Figs. S3-S6, 12).

Wavelet spectra of these four depth series show similar basic patterns of periodicities in the depth domain with all of the thickness periodicities changing in frequency simultaneously (Fig. 2, *SI Appendix,* Fig. S6) reflecting variations in accumulation rate. The most prominent frequency through most of the spectrum reflects the lithologically based McLaughlin Cycle, an expression of the 405 ky orbital eccentricity cycle (Table 2), that provided the basis for time calibration of the N–H APTS (10). The zircon CA-ID-TIMS U-Pb dates from the Newark Basin lava flow formations and related intrusions show a pronounced (nearly order of magnitude: *SI Appendix*, Figs. S6,S11) increase in accumulation rate at the beginning of the CAMP event (Fig. 2), above which the thickness frequencies correspondingly shift to much lower values in agreement with the visual observation of the increased thickness of the McLaughlin Cycles (13,14,15). The borehole geophysical data are complementary to the depth rank data especially where the latter has reduced variability as shown by both wavelet and Multitaper Method (MTM) spectral analysis (Figs. 3,5). MTM analysis of x-ray fluorescence chemical data yield similar results on a subset of the thickness data (*SI Appendix* Figs. S8, S9). We regard this as a powerful verification that the main periodicities can be easily seen in all the depth series by visual inspection without any tuning or nonuniform age model (Fig. 2).

We convert the data from the core depth domain to the time domain with minimal modification using a simple model based on U-Pb dates imported from CPCP-1 via magnetostratigraphy and the lava flows within the section. This yields a spectrum with approximately the expected orbital periodicities (Fig. 4). A prominent cycle at ~405 ky is present. By filtering the core depth series in this range to the thickness of this cycle (*SI Appendix* Fig. S7 and *SI Appendix* Tables S2 and S3) we can determine its period without having to explicitly identify specific lithological McLaughlin Cycles as was done for ref. 12, which confirms the later results with different methods yielding a periodicity of 398±12 ky using all the dates and 410±02 ky using only the three CPCP dates in stratigraphic order and the Newark Basin CAMP dates (*SI Appendix* Fig. S7 and Table S3). Therefore, regardless of the counting methodology, these results are indistinguishable from the 405 ky periodicity predicted to be stable over this time interval (12).

Minimally tuned to the 405 ky periodicity, the wavelet spectra show that all of the frequencies seen in the depth domain are now aligned and the data sets can be directly compared to the spectrum solution for the later Neogene plus Quaternary (Fig. 5, *SI Appendix* Figs. S10,S12). Visual inspection of the wavelet spectra shows overall agreement in pattern in the high power periods except for those longer than 405 ky. In particular, the apparent homologue of the 2.4 My period in the Neogene plus Quaternary wavelet spectrum is distinctly offset to a shorter period of ~1.7 My, ascribed to the Mars-Earth orbital eccentricity Grand Cycle (g_4-g_3) (Table 2) when it was first measured (22,23). The 1.7 My cycle is not visible in the NBCP geophysical logs because of detrending issues with the six down-hole logs from which the composite logs

are assembled (SI Appendix Figs. S2 and S12). The possibility that the difference between this the 1.7 My Triassic period of g_4-g_3 and its present 2.4 My period is due to hiatuses is eliminated by the CPCP-1 and Newark Basin lava flow U-Pb dates (*SI Appendix* Fig. S7 and Tables S2,S3).

Examining the interval between the 405 ky cycle and the 2.4 My cycle in the 0-24 Ma wavelet spectra there are two bands of high power with a "ropy" appearance (Fig. 5: *SI Appendix* Fig. S12). They seem to have their homologues in a similar interval in the depth rank and color wavelet spectra in the Newark-Hartford spectra. These various Grand Cycles seem to correspond to the main terms of the eccentricity orbital solution (see ref. 31, Table 6 and ref.5, Fig. 5: *SI Appendix* Table S4), predicted by combinations of the secular fundamental frequencies (Tables 1-3) these should correspond to the Jupiter-Mercury (g_5-g_1 = 1/972.59 ky) and Venus-Mercury (g_2-g_1 = 1/695.65 ky) cycles (Table 2 and *SI Appendix* Table S4). To our knowledge these have not previously been identified in any geological records. One could argue that because they are different in value from modern frequencies, assignment of these bands of spectral power to specific combinations of astronomical parameters, raises the question of whether they could reflect geological noise or artifacts.

The secular fundamental frequencies of the Solar System.

Fortunately, the question of the origin of the cycles in the Newark-Hartford data set can be convincingly answered using refined Fourier analysis techniques in conjunction with the internal cross checks afforded by the overdetermined components of the orbitally paced cycles themselves (*SI Appendix* Table S7). Multi-Taper-Method (MTM) spectral analysis of the cycles with periods greater than 66 ky previously used for this sequence, has been applied again here (Fig. 6, Table 2, *SI Appendix* Table S4). In addition, we have performed an independent analysis adopting a method developed for the quasiperiodic decomposition of the output of numerical integrations of dynamical systems called "Frequency Analysis" (FA) (28,29) that has been widely used in various domains including experimental physics (30,31). FA automatically extracts the frequencies and amplitudes of the periodic components of a signal, without the need for manual selection of peaks, sorted by decreasing amplitude. We applied FA to the whole Newark-Hartford depth rank data set (200.65 – 225.565 Ma), after removing a 2 My running average using the "TRIP" code (*SI Appendix*). The FA results, limited to the 14 main terms (Table 2), are extremely close to the MTM analysis (Table 2: *SI Appendix* Table S4). Thus, we have obtained the same result using three different approaches (wavelet, MTM, and FA). The FA values will be used hence forth for further quantitative analysis because of its reduced operator-influence.

The MTM and FA analysis of the new Newark-Hartford data exhibit striking similarities in the recovered values to periodic components of Earth's orbital eccentricity in numerical solutions of the past 20 My (compare col. 4 and col. 6 of Table 2) (e.g., ref. 32, Table 6). This is similar to an earlier analysis that predated the independent age model (22). However, the important discrepancies with the past 20 My can now be taken more seriously, the most notable being in the $g_4 - g_3$ argument that has a present period of 2.364 My in the La2010a solution but only 1.747 My in the Newark-Hartford

data. It was argued in (22) that this was the result of chaotic diffusion in the Solar System. We show here that this conclusion is most probably correct with a very high probability.

To a first approximation, the Solar System orbital motion can be considered quasi-periodic, and its long-term evolution can be represented by periodic terms of only 15 main frequencies: the frequencies g_1, $g_{2,...}$ g_8, the secular fundamental frequencies of precession of perihelion of the planets (Mercury, Venus, ..., Neptune), and s_1, s_2, s_3, s_4, s_6, s_7, s_8, the secular fundamental frequencies of precession of the nodes of the orbits of the planets (s_5 is not present due to the conservation of angular momentum). Here the secular frequencies are regarded as an average over 20 My. Insolation quantities on Earth are thus expressed in terms of these secular fundamental frequencies, and additionally the precession frequency of the spin axis of the Earth, *p* (refs. 32, 33, 34). In general, the secular fundamental frequencies do not appear directly in the physical variables, but only as combinations of the frequencies (Tables 1,2: *SI Appendix*: Table S4). For example, in Earth's orbital eccentricity, only differences of the form $g_i - g_j$ are present, and eventually combinations of higher order of the g_i, with a zero sum of the coefficients (see 32). The largest amplitude term in the Earth's orbital eccentricity is the well-known $g_2 - g_5$ = 1/405 ky periodic term. Although the secular fundamental frequencies cannot be measured directly in sedimentary records due to a lack of resolution, the physical effects appear as the differences of frequencies, and, and these secular difference frequencies generate long-period beats that can be measured, with even longer periods than the $g_5 - g_2$ = 1/405 ky term. The geological record can thus be viewed as an interferometer in which the lower, measurable frequencies, the Grand Cycles, can be determined even though the higher frequencies that produce them cannot (Tables 1,2, *SI Appendix* Table S5). We thus can derive the secular fundamental frequencies pertaining to the precession of perihelion g_1 though g_4 directly from the geological data, untethered from current values.

Chaotic diffusion

Although over a few million years the orbital evolution of the Solar System can be approximated by a quasiperiodic motion, as stated above, this is not true extending back in time to 200 Ma, where the chaotic diffusion of the system will be noticeable. The main result will be a small drift in the values of the secular frequencies of the system (5,28,32). This drift is small for individual frequencies, but its effects are greatly amplified in differences of close frequencies (i.e., beat cycles), as in the $g_4 - g_3$, Mars-Earth orbital eccentricity term. The period of this term is at present 2.364 My while the observed value in the Newark Hartford data is apparently only 1.747 My (both FA results, Table 2). Is this possible within the range of the predicted chaotic drift?

To answer this question, we cannot directly integrate back the orbital solution back in time, starting with the present initial conditions. Indeed, due to the chaotic behavior of the Solar System, the uncertainty in the solutions is multiplied by 10 every 10 My, and due to the sensitivity of the gravitational system to perturbations of the largest asteroids (minor planets) Ceres and Vesta, it will never be possible to retrieve precisely the planetary orbits beyond about 60 Ma (35). Nevertheless, the problem can

be addressed in a probabilistic way by integrating the model beyond that time. While this does not provide the exact path of our Solar System, but only a possibility for its past evolution, it does provide a gauge of the reasonableness of the geological data. We thus use 13 orbital solutions of the very precise model of La2004 and La2010 (described in ref. 5) with small variations in the initial conditions compatible with our present knowledge and examine the evolution of the Mars-Earth ($g_4 - g_3$) period from 0-250 Ma (Fig. 7A). The output is analyzed using FA with a sliding window of 20 My with a 1 My offset between each interval (Fig. 7 and *SI Appendix* Figs. S4,S6). Among these 13 solutions, 4 of them, have a ($g_4 - g_3$) period that goes below 1.75 My, and very nearly so for another 4. Thus, finding a 1.75 My value in the geological record in the 200 -225 Ma time interval is entirely compatible with our best knowledge of Solar System motion.

After this first step, we search for a more quantitative estimate. The La2010d solution comes close to the 1.75 My value in nearly the same time interval as the Newark-Hartford data, and we can consider it our reference solution La2010d*. We thus can compare how closely the Newark-Hartford data approximate La2010d* not only for the Mars-Earth ($g_4 - g_3$) cycle but all of the major secular (difference) frequencies for Earth's orbital eccentricity. Direct comparison of the FA results of La2010d* Earth's eccentricity (Table 2 and *Appendix* Table S4) with that of the Newark-Hartford data (Table 2: cols. 4 and 5) shows that the values of the periods are very close, for all of the leading terms of the analyzed data (*SI Appendix* Table S5 and S5). For a quantitative estimate, we use the frequencies expressed as arcsec/yr ("/yr) rather than the period (in yr), because they may be combined in a simpler way (Tables 3 and S4).

Fundamental secular frequencies

We can recover the fundamental secular frequencies from the Newark-Hartford data because of the great stability of the outer Solar System, notably Jupiter. The Newark-Hartford data is tuned to the $g_2 - g_5$ Venus-Jupiter 405 ky term and we expect that FA (and MTM) should recover this value (Table 2, col. 4), which it does. While there is nothing new here, it verifies the consistency of our procedure. In addition, because the outer Solar System is very stable, the g_5 frequency can be considered as a constant over the age of the Earth[1]. Indeed, the g_5 value of La2010d*, obtained with FA, is 4.257438"/yr, extremely close to the La2010a value 4.257482 "/yr of (5). With this assumption, supported by theory and computation, we can recover g_1 from $g_1 - g_5$, g_3 from $g_3 - g_5$, g_4 from $g_4 - g_5$, and g_2 from $g_2 - g_5$. For the last, the fact that we find a value close to the La2010a reference value is expected, due to the tuning to $g_2 - g_5$ (Table 3). The recovered values for g_1, g_2, g_3, g_4 are in the green rows of Table 3, col. 4. We do not compare these values to the La2010a values, but to the ones of La2010d* that should be much closer as it has drifted in a similar way due to chaotic diffusion. Indeed, the differences reported in Table 3, col. 5 are extremely small.

This should be sufficient to give us great confidence that the signal we have recovered in the Newark-Hartford data is actually related to the Earth's orbital eccentricity, but there is much more that can be recovered. Indeed, in the leading terms

[1] The uncertainty in the 405 ky of 1 cycle in 250 Myr being due almost entirely to g_2 (5).

provided by FA, there are 5 additional terms in the FA of the La2010d* eccentricity solution. These terms, $g_4 - g_3$, $g_2 - g_1$, $g_2 - g_5 - (g_4 - g_3)$, $g_3 - g_2$, $g_4 - g_2$, are in the blue rows of Table 3. We use these terms to test the consistency of the results. We compare the values obtained by FA on the Newark-Hartford data to the corresponding combination of the previously determined values for g_1, g_2, g_3, g_4 (with g_5 considered a constant). The differences that are very small are reported as well in col. 5 of Table 3.

The correspondence of the 10 eccentricity terms reported in Table 3 is striking and it is desirable to quantitatively examine whether such a close fit is due to chance. Among these 10 terms, we will not consider g_5 because it is assumed constant. Nor will we consider g_2 because the Newark-Hartford data are tuned to the $g_2 - g_5$ term. We will not also consider $g_4 - g_3$ as we chose the La2010d* solution because $g_4 - g_3$ is close to $g_4 - g_3$ of the Newark-Hartford data early Mesozoic time. There remain 7 frequencies in the Newark-Hartford data that are extremely close to the main La2010d* frequencies. Considering that these 7 frequencies are among the 12 terms of largest amplitude of the Newark-Hartford data (after disregarding the $g_2 - g_5$ and $g_4 - g_3$ terms), we performed a statistical experiment with 33 billion draws of 12 frequencies in the [0,20"/yr] interval. The probability that the close match of the 7 of the 12 terms of the Newark-Hartford to the La2010d* frequencies is due to chance is less than 5×10^{-8} and on the order of 10^{-11} when only 7 frequencies are considered (see *SI Appendix* Figs. S13 and S14). We can thus be very certain that the recovered frequencies in the Newark-Hartford data are actually the secular frequencies of the orbital motion of the Earth, and it is remarkable to see the high precision with which these frequencies are determined (Table 3). While similar values were calculated for the NBCP data in 1999 (22), these new values are much more precise and accurate and pass the stringent tests inherent in the relationships among the secular frequencies, their expression in orbital eccentricity cycles, and their independent U-Pb based age model. It is also the first time, to our knowledge, that such a quantitative statistical assessment has been performed with any geological data with such a convincing result. It is worth noting that the difference between LA2010d* and the Newark-Hartford measurement for the secular fundamental frequency of the precession of perihelion for Mercury of 0.050 ”/yr (Table 3) is nearly an order of magnitude less than the 0.430“/yr contribution of general relativity in the precession of perihelion of Mercury (e.g., Table 4 of refs. 2, 36).

Other geologic expressions of the Mars-Earth ($g_4 - g_3$) cycle in the Newark Basin

The existence of a ~1.75 My cycle in the Triassic age strata of the Newark Basin was first inferred from outcrop data (18), although a 2 My period was estimated at that time. It turns out, based on this current analysis, that intervals of maximum precessional variability at the peaks of this cycle contain all of the formally named members of the vast Passaic Formation, such as the Perkasie Member, originally recognized as distinctive in 1895 (37). These intervals also tend to be the units most easily mapped and units with the most fossils (9), all of which are evidence of the tangibility of these Grand Cycles (*SI Appendix*, Figs. S15 and S16).

Synthetic seismic traces generated from the borehole data of the NBCP show the Grand Cycles (*SI Appendix*, Fig. S15). When tied to deep industry exploratory borehole

records from the Newark basin, themselves tied to seismic lies, both the Jupiter-Venus 405 ky and Mars-Earth 1.75 My cycles can be clearly seen as the most coherent components of the seismic profiles across the basin (38) (*SI Appendix*, Fig. S15). Presumably due to differences in cementation expressed in sonic parameters, the topographic expression of the deeply eroded tilted strata of the Newark basin section also reveals the Grand Cycles which can be seen from space, with ridges reflecting time intervals of high- and valleys low-precessional variability that can be directly tied to the stratigraphy (*SI Appendix*, Fig. S16), much as bundles of plausibly obliquity-related rhythms can be seen in crater walls (39) or polar layered deposits (40) on Mars.

Comparable early Mesozoic results

Thus far, Mesozoic records of astronomical forcing have tended to rely on "floating" astrochronologies or highly tuned records. By designing an experiment in a completely different region, CPCP-1, a globally exportable paleomagnetic and U-Pb based correlative timescale was produced that validated the NH APTS. In so doing, we show the strong fidelity of the 405 ky Jupiter-Venus cycle as predicted by astronomical solutions, which in turn allows us to recognize deviations from current astronomical solutions, extrapolated from the ~60 Ma limit of reliability, especially for the cycles with periods longer than 405 ky.

Pelagic ribbon-chert sequences from Japan have been correlated to the Newark-Hartford data through mainly biostratigraphic webs and carbon isotope stratigraphy. These show remarkable similar periods for the Mars-Earth orbital eccentricity cycle. As with the Newark and Hartford basins, these were deposited in a tropical environment, albeit in the middle of the Panthalassic Ocean (41). In these data, the most prominent low-frequency cycle has a period that varies between 1.8 and 1.6 My, estimated by counting putative climate precession chert-clay couplets. As with the Newark-Hartford data, there does not seem to be any influence of obliquity.

The Early Jurassic age (Hettangian-Sinemurian) epicontinental marine Bristol Channel Basin (United Kingdom) sequence is precession-dominated, expressing eccentricity cycles (42) and has a well-developed astrochronology and paleomagnetic polarity stratigraphy that parallels that in the Newark-Hartford composite. Based on polarity stratigraphy correlation to the Newark-Hartford APTS (43), the 405 ky cyclicity is in phase with that in the Newark-Hartford section and shows an amplitude modulation in phase with the $g_4 - g_3$ cycle in the radioisotopically anchored Newark-Hartford composite (44, 45). Paleomagnetic polarity correlation between the Newark-Hartford composite to the Bristol Channel section and ammonite-based correlation of the Hettangian-Sinemurian boundary from the Bristol Channel section to the marine Pucara Group (Peru) allows zircon U-Pb ages to be exported to the Bristol Channel and the Newark-Hartford Jurassic sections. The Pucara section has many zircon U-Pb CA-ID-TIMS dated ash layers with ages (46,47) in agreement with both the Newark-Hartford and Bristol Channel Basin astrochronologies (44). An alternation in intensity of cycles attributed to climatic precession suggests a hint of obliquity pacing in the Bristol Channel data (43) consistent with its higher-latitude position during the Early Jurassic (~32°N) relative to the Newark-Hartford record (~21°N) (10). A similar, stronger

indication of obliquity are in results from higher latitude, Rhaetian coal-bearing sequences of the Sichuan basin China (48).

Comparison to the Cenozoic and search for obliquity modulation

Comparisons of the recent compilation of benthic foraminifera $\delta^{18}O$ data "Megasplice" (49) and modulators of obliquity to the astronomical solution for eccentricity and the Newark data are informative (Figs. 5 and 6). The wavelet spectrum of the $\delta^{18}O$ benthic Megasplice has a less resolved structure than the Newark data. This is seen also in the MTM spectrum. The short orbital eccentricity cycles are well-resolved as is the Jupiter-Venus 405 ky cycle; however, all of these cycles were used in tuning the geologically older records that comprise the Megasplice, while geologically younger parts used an age model (LR04: ref. 50,49) in which an ice model incorporating the La93 solution (51), was used to tune the individual records that make up the LR04 stack, therefore their agreement with the orbital solutions is not independent. The obliquity modulating cycles (Fig 6D) are like the eccentricity cycles in that all of the frequencies are combination tones of s_1, s_2,…s_5, which are related to precession of the node of each planetary orbit (e.g., s_5 is related to the precession of the nodes of the orbit of Jupiter). We can even use the term Grand Cycles of obliquity to refer to the ensemble of long period cycles.

The MTM spectrum of obliquity shows what should be expected in the Newark or $\delta^{18}O$ benthic mega-splice if obliquity were a major component of the records. There is no obvious signal that can be assigned to combinations of the Grand Cycle s_1, s_2,…s_5 secular frequencies in the Newark-Hartford data, although there could be confusion between the obliquity cycles around 100 ky and the short eccentricity cycles. Surprisingly, however, there is also no clear obliquity signal in the MTM spectrum of the $\delta^{18}O$ benthic Megasplice as represented here either, even though some beats, especially the 1.2 My (s_4–s_3) Grand Cycle are evident in the wavelet spectrum and they have been reported from the older components of the $\delta^{18}O$ benthic Megasplice, not examined here, and used to constrain astronomical solutions (52,53). Based on the wavelet spectrum, the obliquity Grand Cycles are smeared out in the younger part of the Megasplice record. This is despite the fact that obliquity and its longer period modulators are known to be a significant part of the pacing of climate as seen in some of the records making up the Megasplice and high-latitude non-marine records (e.g., 52,53,54,55). Whether this reflects real aspects of the climate system, perhaps dampened by low CO_2, mixing of signals from different parts of the climate system, the $\delta^{18}O$ proxy itself, or issues with tuning requires much additional work.

Grand cycles and the roadmap to Solar System chaos

The results from the wavelet, MTM spectra and FA of the Newark-Hartford data (Figs. 5 and 6 and Table 2 and 3) are remarkable, because while the calculations of the Grand Cycles from the short eccentricity cycles in the 0-22 Ma data is due to their necessary linkage in the way the astronomical solution is deconvolved and the secular

frequencies are resolved, the succession of rock layers 210 million years old has no such necessary linkage: it can only result from the sedimentary record of the climate response to the same physics that are imbedded in the 0-22 Ma eccentricity solution playing out in time. The differences between the current g_1, g_2, g_3, g_4 values (Table 3, col. 7) and their Newark-Hartford FA determinations (Table 3, col. 4) are therefore significative and most parsimoniously explained as the result of chaotic diffusion in the gravitational interactions of the Solar System. In particular, the drift of $g_4 - g_3$ from the 2.36 My present value to the 1.75 My period observed in the NH data can be considered as a direct geological evidence of the chaotic behavior of the Solar System.

Strong evidence for Grand Cycle orbital eccentricity pacing of climate is widespread in the lower latitudes during the Late Triassic and Early Jurassic. However, the results presented here suggest that the present astronomical solution for eccentricity do not fit the frequency data well for this time period (*Table 3*). We found a good match with the La2010d* solution, but it is expected that a more systematic search of the possible variations of the astronomical solutions could lead to an even better match. The very new and important result for the Newark-Hartford data is to provide precise values for the Triassic-Jurassic secular fundamental frequencies g_1, g_2, g_3, g_4 that could be considered as reference point and used as an anchor for the search of orbital solutions that could match the past orbital evolution of the Solar System, as recorded in the sedimentary data.

However, a major contributor to the chaotic behavior, in fact its signature (2), is related to the Mars-Earth secular resonance $(g_4 - g_3) - 2(s_4 - s_3)$ (now in libration, i.e., oscillation in phase space) and its possible transitions to and from $(g_4 - g_3) - (s_4 - s_3)$ (circulation, i.e., rotation in phase space), with the resulting 2:1 vs 1:1 periods of the eccentricity and obliquity Grand Cycles (Figure 7A). Because the Newark-Hartford data show no clearly discernible obliquity pacing, the mode of 2:1 vs 1:1 resonance in the secular frequencies cannot presently be determined for this time interval. While there has been some recent progress with tantalizing results (56), the transition from the 2:1 vs 1:1 periods has yet to be unambiguously observed in suitably long records, and it is possible that it has never occurred although most numerical solutions show it. To obtain a result for the Triassic-Jurassic secular resonance, suitably long (>10 My) contemporaneous high-latitude records that would be expected to show a strong obliquity pacing are needed. For example, the continental and coal-bearing, Triassic-Jurassic ~70°N Junggar Basin section shows strong hints of obliquity forcing interpreted to be a 2:1 ratio of eccentricity to obliquity Grand Cycles (~1.6:0.8 Ma), but that section lacks an independent geochronologic or paleomagnetic polarity timescale, although it does exhibit 405 ky periodicity (44). Cores spanning 10s of millions of years from such a section would permit a high-resolution paleomagnetic polarity record to be developed from the basin (extremely difficult to do in outcrop in these gray and black strata because of weathering) that would allow correlation to the Newark-Harford data and presumably resolve the mode of resonance in the eccentricity and obliquity Grand Cycles. This would be a full proof-of-concept of the Geological Orrery.

If the resonance is in the 2:1 ratio for the latest Triassic and earliest Jurassic, as the preliminary interpretations suggests, this finding would only apply to that particular time, and we still cannot show when or if the 1:1 situation ever happens. There are strong hints that even longer astronomical cycles with periods of ~8-9 My and ~36 My

(41,57) that may modulate the Grand Cycles and these modulations could be confused with actual changes in secular frequencies or tectonic influences in records that are too short. To examine these potential empirical phenomena will require careful concatenation of multiple long records with appropriate properties, including independent geochronology, all accurately recording low and high frequencies that pass the types of rigorous tests outlined here.

A complete Geological Orrery would consist of multiple sets of paired low- and high-latitude records (preferably cored to ensure superposition and continuity), spanning the Paleogene to Permian and beyond, with even deeper time highly desirable. When combined with the existing record from the last ~60 My, the last ~250 My of Solar System history would be covered. The empirical mapping of the secular frequencies of the Grand Cycles in eccentricity and obliquity over this time interval (including the transitions in secular resonances, should they occur) would constitute an entirely new empirical realm to test Solar System evolution, astronomical solutions, and gravitational models. By constraining the past evolution of the speed of perihelion of Mercury g_1, the results would provide mechanisms to constrain the evolution of the flattening parameter J_2 of the Sun and further test General Relativity and its alternatives (3).The constraint on the past evolution of the other secular frequencies may be used to limit the existence of additional planets, and examine predictions of galactic disk dark matter interactions with the Solar System (57,58). The results would also be important in efforts to tune radiometric decay constants for geochronology and to produce accurate solar insolation targets beyond 60 Ma.

Materials and methods

Core used in this analysis originate from three sedimentary basins in North America (Fig. S1): the cores from the 7 NBCP core sites (Newark Basin); the ACE cores(Newark Basin); the Silver Ridge Core (Hartford Basin); the Park River Cores (Hartford Basin); the MDC cores, and the CPCP-PFNP13-1A core (Colorado Plateau). Details of locations are given in the Supplementary Information (*SI Appendix*, Table 1).

MTM spectra (Figs. 3, 4, 6; and *SI Appendix*, Fig. S9) were developed using Analyseries (2.0) which was also used for filtering, interpolation, etc. (59), and the wavelet spectra (Figs. 2, 3, 5 and Figs. S6 and S12) were computed using the Matlab script of Torrence and Compo (60) (paos.colorado.edu/research/wavelets/). For all data, Analyseries (2.0) was used for interpolation and for the time series based on the Laskar 2004 solution (32), which in the case of the last 0-24 Ma, is not significantly different from more recent solutions (5). The Frequency Analysis (FA) method is described in refs. 28,29, and has been used with its implementation in the TRIP software, that is documented and freely available at www.imcce.fr/trip/. The TRIP source code used in this work is given in the SI. Work on the NBCP and CPCP cores was conducted at the Rutgers Core Repository as described in ref. (12) and CPCP core analysis and documentation was conducted at the LacCore facility at the University of Minnesota (11).

ACKNOWLEDGMENTS. We express our gratitude for the encouragement and guidance of NSF program directors Leonard Johnson and the late Richard Lane leading up to and during the funded phases of the Newark Basin Coring Project and the Colorado Plateau Coring Projects, respectively. We thank Randy Steinen for access to the new MDC cores of the Hartford Basin and Margret Thomas and Randy Steinen for access to the Park River cores. We thank the National Park Service, particularly superintendent Brad Traver, for permission to core, and William Parker for encouragement and advice during coring and the pre-drilling workshops. This project was funded by National Science Foundation (NSF) grant EAR 8916726 to (to P.E.O. and D.V.K.) for the NBCP, and for the CPCP, by collaborative Grants EAR 0958976 (to P.E.O), and 0958859 (to D.V.K.), and ICDP (International Scientific Continental Drilling Program grant 05-2010, and. P.E.O. and S.T.K. acknowledge support from the Lamont-Climate Center, and D.V.K. is grateful to the Lamont–Doherty Incentive Account for support of the Paleomagnetics Laboratory. S.T.K. acknowledges support from the NSF Graduate Research Fellowship Program Grant DGE 16-44869. J.L. acknowledges support from the PNP Program of Planetology and from the Paris Observatory Scientific Council. Curatorial facilities for the work halves of the CPCP cores and all of the Newark Basin NBCP and ACE cores are provided by the Rutgers Core Repository. For access to the curatorial facilities for the ACE and MCD ACE cores we thank James Browning and Randolph Steinen, and for access to the Park River ACE cores we thank Margaret Thomas and Randolph Steinen. We also thank Clara Chang for help with ITRAX data collection and processing. The senior author completed this paper while on sabbatical as a visiting scientist at Amherst College's Beneski Museum, for which he is grateful. This work was partly supported by the National Natural Science Foundation of China (41730317), Special Basic Program of Ministry of Science and Technology of China (2015FY310100), Bureau of Geological Survey of China and the National Committee of Stratigraphy of China (DD20160120-04). Any opinions, findings, or conclusions of this study represent the views of the authors and not those of the US Federal Government. This is a contribution to UNESCO-IUGS IGCP-632, and is Petrified Forest Paleontological Contribution XX, and Lamont–Doherty Earth Observatory Contribution XXXX.

Figures

Figure 1: Map of Pangea at ~200 Ma with locations discussed in text.

Figure 2: Untuned depth-domain wavelet spectra from the Newark-Hartford data set. The cores, holes, and outcrops that are described in the *SI Appendix* (Fig. S1, Table. S1). Crucial are the demonstrable and simultaneous shifts in all thickness periods, particularly pronounced in the lower two-thirds of the record in all spectra. There is a nearly order of magnitude increase in accumulation rate above the lowest Basalt (OM) at 0 m. Red horizontal lines mark the positions of the following lava flow formations of the CAMP; OM, Orange Mt. Basalt (Talcott Basalt in Hartford Basin); P, Preakness Basalt (Holyoke Basalt in Hartford Basin); HM, Hook Mt. Basalt (Hampden Basalt in Hartford Basin). Zircon U-Pb CA-ID-TIMS ages are: 1, based on paleomagnetic correlation to Bristol Channel Basin Hettangian-Sinemurian Boundary at GSSP (43,44) and then to the Pucara Group via ammonite biostratigraphy (43,46)]; 2, 200.916 ± 0.068 Ma [Butner intrusion related to Hook Mt. Basalt (21)]; 3, 201.274 ± 0.032 Ma [Preakness Basalt (21)]; 4, 201.520 ± 0.034 Ma [(Palisade Sill feeder to Orange Mt. Basalt (21)]; 5, 210.08 ± 0.22 Ma; 6, 213.55 ± 0.28 Ma; 7, 212.81± 1.25 Ma; 8. 214.08 ± 0.20 Ma. 5 – 8 are all Chinle Formation (12).

Figure 3: Comparison between untuned depth rank data from core and reflection coefficient data (derived from borehole sonic velocity and density measurements (61) from the Rutgers and Somerset cores and holes of the NBCP (see SI) showing their similarity in periodicities and complementarity and stratigraphic positions of zircon ages. The reflection coefficient is thus different than the sonic velocity logs shown on other figures. The interval from ~1530 m to ~1640 m lacks structure in depth ranks but shows clear periodicities similar to surrounding strata in the reflection coefficient data. A, Comparison of wavelet spectra showing very similar structure and periodicities. B, MTM spectra of depth rank and reflection coefficient data showing very similar cyclicity attributed to orbital eccentricity, as well as the average f-statistic (values greater than 0.7 for both data sets. The “F-test” axis label refers to the F-test significance level. Analyseries 2.0 default: 6, 4pi tapers) and Blackman-Tukey coherence between the two data sets (Analyseries 2.0 default: 30% autocorrelation; 80% confidence level). Note the close correspondence between frequencies with high coherence, high statistical significance, and high power. See SI for details.

Figure 4: Simple age model for untuned NBCP data using zircon U-Pb CA-ID-TIMS dates from basalt flows in the Newark Basin section (21) and CPCP dates projected onto the Newark Basin section using paleomagnetic polarity correlations (12). This shows that available dates are incompatible with significant gaps in the section. Vertical gray bars guide the eye to the periods from the La2004 solution of 0-22 Ma with period shown in a smaller font at the top of 4C – shown for reference. A, Accumulation rate determined by using the Orange Mt. Basalt date (21) in contact with the top of the NBCP data and the three CPCP dates with small uncertainties (12) – uncertainty magnitude shown by diameter of point: O, Orange Mt. Basalt (Palisade Sill); P, Preakness Basalt; H, Hook Mt. Basalt (Butner intrusion); 52Q-1, 185Q-2, 182Q-1,

CPCP dates; 177Q-1, CPCP date with large uncertainty and not used. B, Duration of cycle thought to represent the 405 ky cycle based on counting long wavelength (~60 m) filtered cycles from untuned NBCP depth rank data (*SI Appendix* Fig S7, Table S3): same abbreviations as follow those in panel A. C, MTM spectrum (using width-ndata product=4 and 6 windows options of Analyseries 2.0) of untuned sequence of NBCP depth ranks over the interval with independent dates showing the prominent period at ~405 ky based on the age model in A, along with the cluster of significant periods at high power close to the anticipated period of the short eccentricity cycle, as well as at a period close to the anticipated period of the Mars-Earth Grand Cycle. D, MTM spectrum (Analyseries 2.0 default 6, 4pi tapers) of untuned sequence of NBCP sonic velocity (from boreholes) showing the prominent period at ~405 ky based on the age model in A, along with the cluster of significant periods at high power close to the anticipated period (averaging ~100 ky of the short eccentricity cycle. For C and D, the "F-test" axis label refers to the F-test significance level.

Figure 5: Comparison of time domain wavelet spectra of similar length from the Newark-Hartford data set and the last ~24 million years of the Neogene and Quaternary (δ^{18}O Megasplice) for the, all processed the same way [see SI for details). The Newark-Hartford periods homologous to those in the precession index are apparent, as is the difference in the Mars-Earth cycle between the more ancient and the modern solution. Note periodicities at the lower frequencies show up as pulsing in amplitude in the higher frequencies. Precession is derived from clipped precession index of Laskar 2004 (32) and the δ^{18}O Megasplice is from ref 49.

Figure 6: Comparison of MTM (Analyseries 2.0 default: 6, 4 pi tapers) spectra from the 0-22 Ma Laskar 2004 solution for eccentricity (32), 405 ky tuned Newark-Hartford depth rank data, the δ^{18}O benthic Megasplice (49), and clipped Laskar 2004 solution for obliquity (32). A 0-22 Ma interval instead of 0-24 Ma (as in the color data in Fig. 3) was used because this is the same length as the depth rank data, as opposed to the 0-24 Ma interval in the color data (Fig. 3) The periods (in ky) above each spectrum are labeled where there is both high power and a high f-significance level. The thick, vertical gray bands highlight key frequencies of eccentricity spectrum. The small differences between the eccentricity solution and the Newark-Hartford data are regarded as meaningful (see text and Table 2). The Newark-Hartford data are tuned only to the 405 ky Jupiter-Venus cycle ($g_2 - g_5$), while the δ^{18}O benthic Megasplice (49) is a composite of several tuned records individually tuned to a suite of periodicities including all the major eccentricity periods from 405 to ~100 ky for the older records and obliquity and matching to the LR03 stack for the younger ones (as described in SI in ref. 49).

Figure 7. Evolution of the period of the $g_4 - g_3$ and $s_4 - s_3$ terms in 13 numerical solutions of the Solar System, integrated over 250 My in the past. Values of the frequencies are obtained by Frequency Analysis (FA) over a sliding time interval of 20 My, with an offset of 1 My between each interval. (A) the period of $s_4 - s_3$ is plotted with respect to the $g_4 - g_3$ period. The black line corresponds to the 2:1 resonance ($P(g_4 - g_3) = 2P(s_4 - s_3)$, where P is period of) while the red line is the 1:1 resonance ($P(g_4 - g_3) = P(s_4 - s_3)$). The green circle at (2.4,1.2) is the present value for the Solar System

and starting point of all solutions. (B) $P(g_4 - g_3)$ is plotted over time for all 13 solutions. The black curve corresponds to La2010d (5). The red curve is the La2004 (32). In both A, B the green line is $P(g_4 - g_3)$=1.75 My, the observed value in the Newark-Hartford data.

References

1. Laplace P-S, M de (1812) *Théorie analytique des probabilités*, (Courcier Paris), 464 p.
2. Laskar J (1999) The limits of Earth orbital calculations for geological time-scale use. *Phil Trans Roy Soc Lond (A)* 357(1757):1735–1759.
3. Laskar, J. (2003) Chaos in the Solar System. *Ann Henri Poincaré* 4(2):693–705.
4. Pälike H, Laskar J, Shackleton N (2004) Geologic constraints on the chaotic diffusion of the solar system. *Geology* 32(11):929–93a.
5. Laskar J, Fienga A, Gastineau M, Manche H (2011) La2010: A new orbital solution for the long-term motion of the Earth. *Astron Astrophys* 532(A89):1–15.
6. Buick T (2013) *Orrery: A Story of Mechanical Solar Systems, Clocks, and English Nobility*, (Springer-Verlag New York), 299 p.
7. Applegate JH, Douglas MR, Gürsel Y, Hunter P, Seitz C, Sussman GJ (1986) A digital Orrery. *The Use of Supercomputers in Stellar Dynamics*, eds Hut P, McMillan SL (Springer Berlin, Heidelberg) pp. 86–95.
8. Sussman GJ, Wisdom J (1992) Chaotic evolution of the solar system. *Science* 257(5066):56–62.
9. Olsen PE, Kent DV, Cornet B, Witte WK, Schlische RW (1996) High-resolution stratigraphy of the Newark rift basin (early Mesozoic, eastern North America). *Geol Soc Am Bull* 108:40–77.
10. Kent DV, Olsen PE, Muttoni G (2017) Astrochronostratigraphic polarity time scale (APTS) for the Late Triassic and Early Jurassic from continental sediments and correlation with standard marine stages. *Earth Sci Rev* 166:153–180.
11. Olsen PE, et al. (2018) Colorado Plateau Coring Project, Phase I (CPCP-I): A continuously cored, globally exportable chronology of Triassic continental environmental change from Western North America. *Scientific Drilling* 24:15–40.
12. Kent DV, et al. (2018) Empirical evidence for stability of the 405 kyr Jupiter-Venus eccentricity cycle over hundreds of millions of years. *PNAS* /doi/10.1073/pnas.1800891115.
13. Olsen PE, Schlische RW, Fedosh MS (1996) 580 ky duration of the Early Jurassic flood basalt event in eastern North America estimated using Milankovitch cyclostratigraphy. *The Continental Jurassic* Morales M, ed (Museum of Northern Arizona Bulletin 60), pp. 11–22.
14. Whiteside JH, Olsen PE, Kent DV, Fowell SJ, Et-Touhami M (2007) Synchrony between the CAMP and the Triassic-Jurassic mass-extinction event? *Palaeogeogr Palaeoclimatol Palaeoecol* 244(1-4):345–367.
15. Kent DV, Olsen PE (2008) Early Jurassic magnetostratigraphy and paleolatitudes from the Hartford continental rift basin (eastern North America): Testing for

polarity bias and abrupt polar wander in association with the Central Atlantic Magmatic Province. *J Geophys Res* 113:B06105.
16. Kent DV, Tauxe L (2005) Corrected Late Triassic latitudes for continents adjacent to the North Atlantic. Science 307(5707):240–244.
17. Van Houten FB (1964) Cyclic lacustrine sedimentation, Upper Triassic Lockatong Formation, central New Jersey and adjacent Pennsylvania. *Symposium on Cyclic Sedimentation* Mermiam OF, ed (Kansas Geological Survey Bulletin 169) pp. 497–531.
18. Olsen PE (1986) A 40-million-year lake record of early Mesozoic climatic forcing. *Science* 234:842-848.
19. Olsen PE, Kent DV (1996) Milankovitch climate forcing in the tropics of Pangea during the Late Triassic. *Palaeogeogr Palaeoclimatol Palaeoecol* 122:1–26.
20. Kent DV, Olsen PE, Witte WK (1995) Late Triassic-earliest Jurassic geomagnetic polarity sequence and paleolatitudes from drill cores in the Newark rift basin, eastern North America. *J Geophys Res* 100:14965–14998.
21. Blackburn TJ, et al. (2013) Zircon U–Pb geochronology links the end-Triassic extinction with the Central Atlantic Magmatic Province. *Science* 340:941–945.
22. Olsen PE, Kent DV (1999) Long-period Milankovitch cycles from the Late Triassic and Early Jurassic of eastern North America and their implications for the calibration of the Early Mesozoic time-scale and the long-term behaviour of the planets. *Phil Trans R Soc Lond A* 357:1761–1786.
23. Olsen PE (2001) Grand cycles of the Milankovitch band. Eos Tran Amer Geophys Union Sup 82(47) Abstract U11A-11, p. F2.
24. Hilgen FJ, Krijgsman W, Langereis CG, Lourens LJ (1997) Breakthrough made in dating of the geological record. *EOS Trans Amer Geophys Union* 78(28):285-289,
25. Tanner LH, Lucas SG (2015) The Triassic-Jurassic strata of the Newark Basin, USA: a complete and accurate astronomically-tuned timescale? *Stratigraphy* 12:47-65.
26. Van Veen PM (1995) Time calibration of Triassic/Jurassic microfloral turnover, eastern North America – comment. *Tectonophysics* 245:93–95.
27. Kozur H, Weems RE (2005) Conchostracan evidence for a late Rhaetian to early Hettangian age for the CAMP volcanic event in the Newark Supergroup, and a Sevatian (late Norian) age from the immediately underlying beds. *Hallesches Jahrb Geowiss* B27:21–51.
28. Laskar J (1990) The chaotic motion of the Solar System : a numerical estimate of the size of the chaotic zones. *Icarus* 88, 266-291. .
29. Laskar J (2005) Frequency Map analysis and quasi periodic decompositions, in *Hamiltonian systems and Fourier analysis*, Benest D, Froeschle C, Lega E, eds, Taylor and Francis.
30. Robin D, Steir C, Laskar J, Nadolski L (2000) Global dynamics of the Advanced Light Source (ALS) revealed through experimental Frequency Map Analysis. *Phys Rev Let* 85(3):558-561.
31. Laskar J (2003) Frequency map analysis and particle accelerators. *Proceedings of the 2003 Particle Accelerator Conference, Volume 1* (IEEE, Portland) pp. 378-382.

32. Laskar J, et al. (2004) A long-term numerical solution for the insolation quantities of the Earth. *Astron Astrophys* 428(1):261-285.
33. Berger A, Loutre MF, Laskar J (1992) Stability of the Astronomical Frequencies Over the Earth's History for Paleoclimate Studies. *Science* 255(5044):560-566.
34. Berger A, Loutre MF (1990) Origine des fréquences des éléments astronomiques intervenant dans le calcul de l'insolation. *Bull Class Sci (Acad Roy Belg) ser 6* 1(1-3):45-106.
35. Laskar J, Gastineau M, Delisle J-B, Farres A, Fienga A (2011) Strong chaos induced by close encounters with Ceres and Vesta. *Astron Astrophys* 532:L4.
36. Will, C.M. (2006) The Confrontation between General Relativity and Experiment, Living Rev Relativ 9:3, https://link.springer.com/article/10.12942/lrr-2006-3
37. Lyman BS (1895) New Red of Bucks and Montgomery Counties, [Pennsylvania]. in Final report ordered by legislature, 1891; a summary description of the geology of Pennsylvania (Pennsylvania Geological Survey 3(2):2589-2638.
38. Reynolds DJ (1993) *Sedimentary Basin Evolution: Tectonic and Climatic Interaction*. [Ph.D. thesis]: New York, New York, Columbia University, Department of Earth and Environmental Sciences, 215 p.
39. Lewis KW et al. (2008) Quasi-periodic bedding in the sedimentary rock record of Mars. *Science* 322(5907):1532-1535.
40. Laskar J, Levrard B, Mustard J (2002) Orbital forcing of the Martian polar layered deposits. *Nature* 419:375-377.
41. Ikeda M, Tada R (2013) Long period astronomical cycles from the Triassic to Jurassic bedded chert sequence (Inuyama, Japan); Geologic evidences for the chaotic behavior of solar planets. *Earth Planets Space* 65(4):351–360.
42. Ruhl M, et al. (2010) Astronomical constraints on the duration of the early Jurassic Hettangian stage and recovery rates following the end-Triassic mass extinction (St. Audrie's Bay/East Quantoxhead, UK). *Earth Planet Sci Lett* 295:262–276.
43. Hüsing SK, et al. (2014) Astronomically-calibrated magnetostratigraphy of the Lower Jurassic marine successions at St. Audrie's Bay and East Quantoxhead (Hettangian–Sinemurian; Somerset, UK). *Palaeogeogr Palaeoclimatol Palaeoecol* 403:43–56.
44. Sha J, Olsen PE, Xu D, Yao X, Pan Y, Wang Y, Zhang X, Vajda V (2015) Early Mesozoic, high-latitude continental Triassic–Jurassic climate in high-latitude Asia was dominated by obliquity-paced variations (Junggar Basin, Urumqi, China). *PNAS* 112(12):3624–3629.
45. Xu W, Ruhl M, Hesselbo SP, Riding JB, Jenkyns HC (2017) Orbital pacing of the Early Jurassic carbon cycle, black-shale formation and seabed methane seepage. *Sedimentology 64*(1):127-149.
46. Guex J, et al. (2012) Geochronological constraints on post-extinction recovery of the ammonoids and carbon cycle perturbations during the Early Jurassic. *Palaeogeogr Palaeoclimatol Palaeoecol* 346:1–11.
47. Yager JA, et al. (2017) Duration of and decoupling between carbon isotope excursions during the end-Triassic mass extinction and Central Atlantic Magmatic Province emplacement. *Earth Planet Sci Lett* 473:227–236.

48. Li M, Zhang Y, Huang C, Ogg J, Hinnov L, Wang Y, Zou Z, Li L. (2017) Astronomical tuning and magnetostratigraphy of the Upper Triassic Xujiahe Formation of South China and Newark Supergroup of North America: implications for the Late Triassic time scale. Earth and Planetary Science Letters. 475:207–223.
49. De Vleeschouwer D, Vahlenkamp M, Crucifix M, Pälike H (2017) Alternating Southern and Northern Hemisphere climate response to astronomical forcing during the past 35 m.y. *Geology* 45(4):375-378.
50. Lisiecki LE, Raymo ME (2005) A Pliocene-Pleistocene stack of 57 globally distributed benthic $\delta^{18}O$ records. Paleoceanography 20, PA1003, doi:10.1029/2004PA001071.
51. Laskar JF, Joutel F, Boudin F (1993) Orbital, precessional and insolation quantities for the Earth from -20 Myr to +10 Myr. *Astron Astrophys* 270:522– 533.
52. Pälike H, Laskar J, Shackleton NJ (2004) Geologic constraints on the chaotic diffusion of the Solar System. *Geology* 32(11):929-932.
53. Pälike H, et al. (2006) The heartbeat of the Oligocene climate system. *Science* 314(5807):1894-1898.
54. Dam JA et al. (2006) Long-period astronomical forcing of mammal turnover. *Nature* 443:687-691.
55. Prokopenko AA et al. (2006) Orbital forcing of continental climate during the Pleistocene: a complete astronomically tuned climatic record from Lake Baikal, SE Siberia. Quaternary Science Reviews 25(23):3431–3457.
56. Ma C, Meyers SR, Sageman BB (2017) Theory of chaotic orbital variations confirmed by Cretaceous geological evidence. *Nature* 542(7642):468–470.
57. Boulila S, et al. (2018) Long-term cyclicities in Phanerozoic sea-level sedimentary record and their potential drivers. *Global and Planetary Change* 165:128-136.
58. Rampino MR (2015) Disc dark matter in the Galaxy and potential cycles of extraterrestrial impacts, mass extinctions and geological events. Monthly Notices Roy. Astron Soc 448(2):1816-1820.
59. Paillard D, Labeyrie L, Yiou P (1996) Macintosh program performs time-series analysis. Eos Trans AGU 77:379.
60. Torrence C, Compo GP (1998) A practical guide to wavelet analysis. Bull Am Meteorol Soc 79:61–78.
61. Ramsey M (technical writer) (2018) Schlumberger Oilfield Glossary. https://www.glossary.oilfield.slb.com/en/Terms/r/reflection_coefficient.aspx

Figure 1

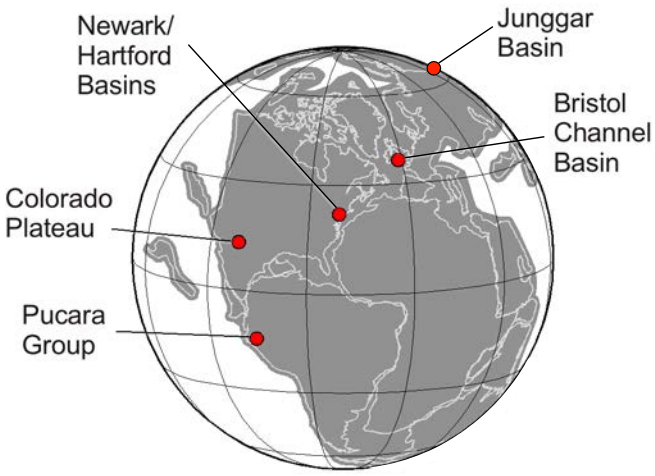
Newark/
Hartford
Basins
Junggar
Basin
Bristol
Channel
Basin
Colorado
Plateau
Pucara
Group

Figure 2

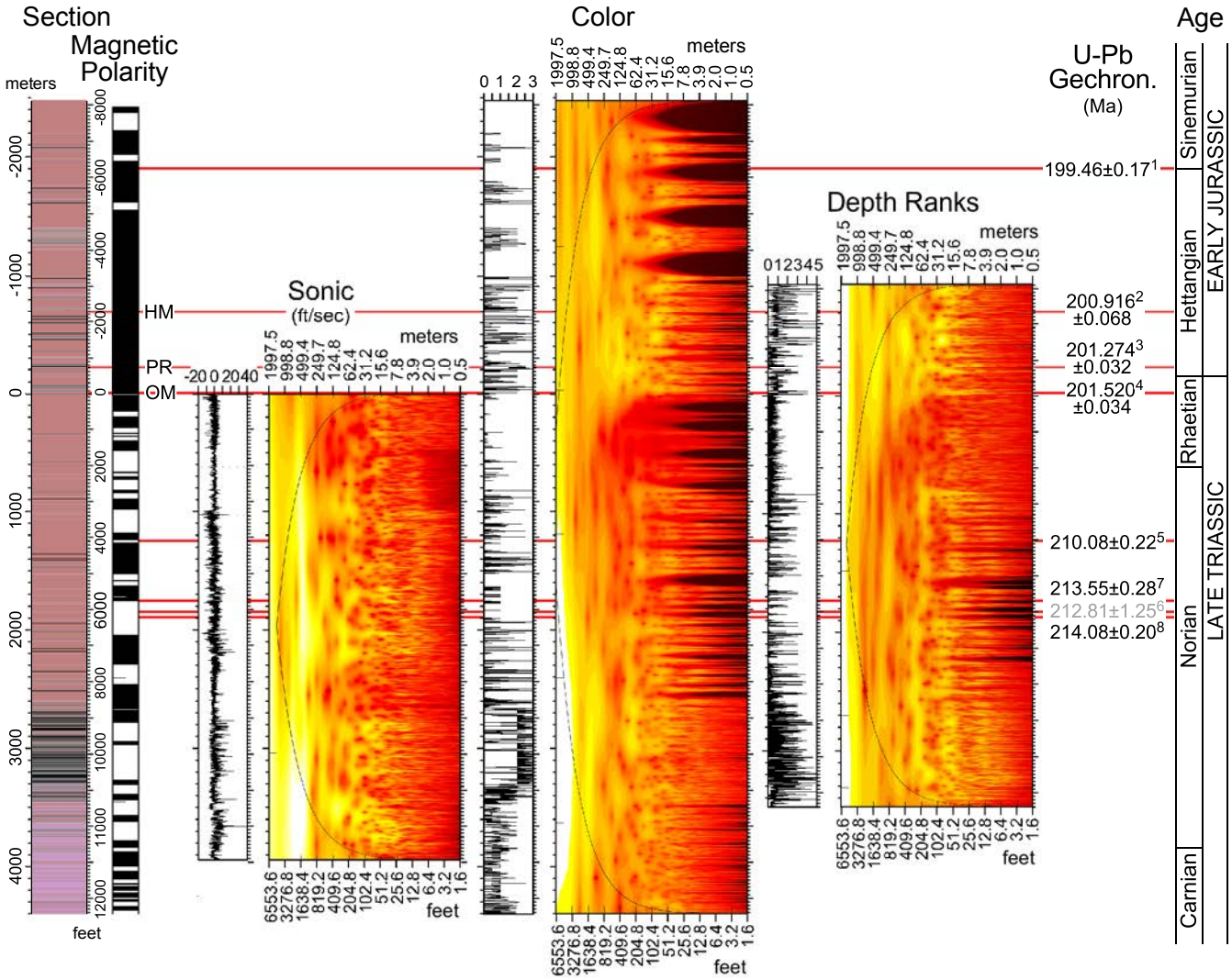
Section
Magnetic Polarity
meters
feet
HM
PR
OM
Sonic
(ft/sec)
-20 0 20 40
meters
feet
Color
0 1 2 3
meters
feet
Depth Ranks
0 1 2 3 4 5
meters
feet
U-Pb Gechron.
(Ma)
199.46±0.17[1]
200.916[2] ±0.068
201.274[3] ±0.032
201.520[4] ±0.034
210.08±0.22[5]
213.55±0.28[7]
212.81±1.25[6]
214.08±0.20[8]
Age
Sinemurian
Hettangian
Rhaetian
Norian
Carnian
EARLY JURASSIC
LATE TRIASSIC

Figure 3

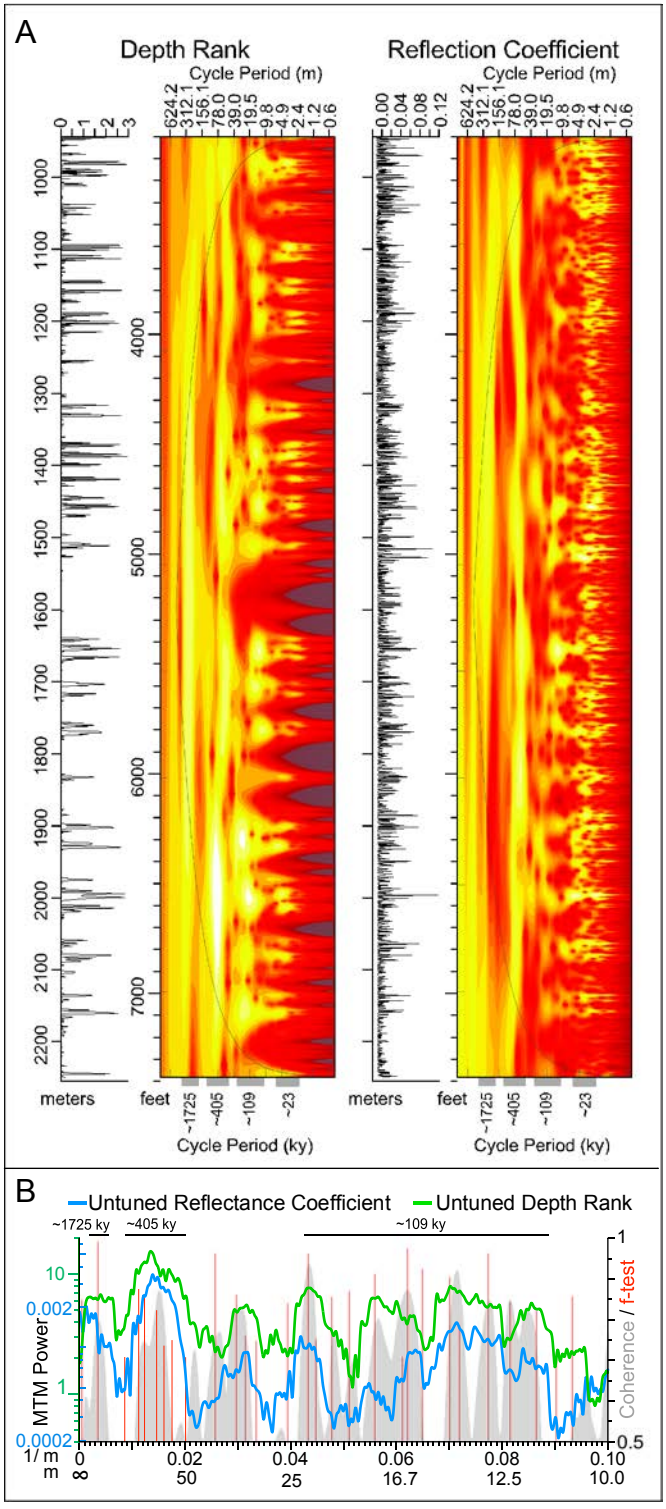
A
Depth Rank
Reflection Coefficient
Cycle Period (m)
624.2
312.1
156.1
78.0
39.0
19.5
9.8
4.9
2.4
1.2
0.6
meters
feet
~1725
~405
~109
~23
Cycle Period (ky)
B
Untuned Reflectance Coefficient
Untuned Depth Rank
~1725 ky
~405 ky
~109 ky
MTM Power
Coherence / f-test
1/ m
m
0
0.02
0.04
0.06
0.08
0.10
50
25
16.7
12.5
10.0

Figure 4

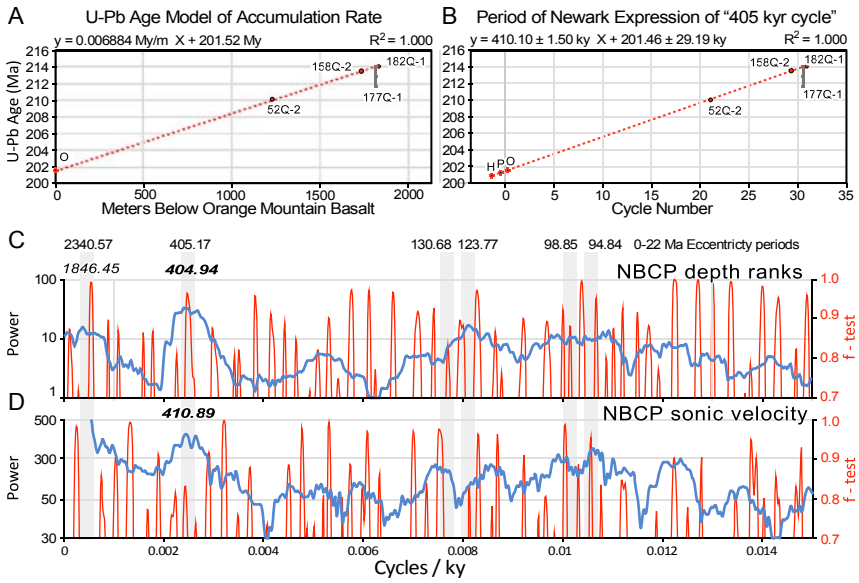
A
U-Pb Age Model of Accumulation Rate
y = 0.006884 My/m X + 201.52 My
R2 = 1.000
U-Pb Age (Ma)
Meters Below Orange Mountain Basalt
158Q-2
182Q-1
177Q-1
52Q-2
O
B
Period of Newark Expression of "405 kyr cycle"
y = 410.10 ± 1.50 ky X + 201.46 ± 29.19 ky
R2 = 1.000
Cycle Number
H
P
O
C
2340.57
405.17
130.68
123.77
98.85
94.84
0-22 Ma Eccentricty periods
1846.45
404.94
NBCP depth ranks
Power
f - test
D
410.89
NBCP sonic velocity
Cycles / ky

Figure 5

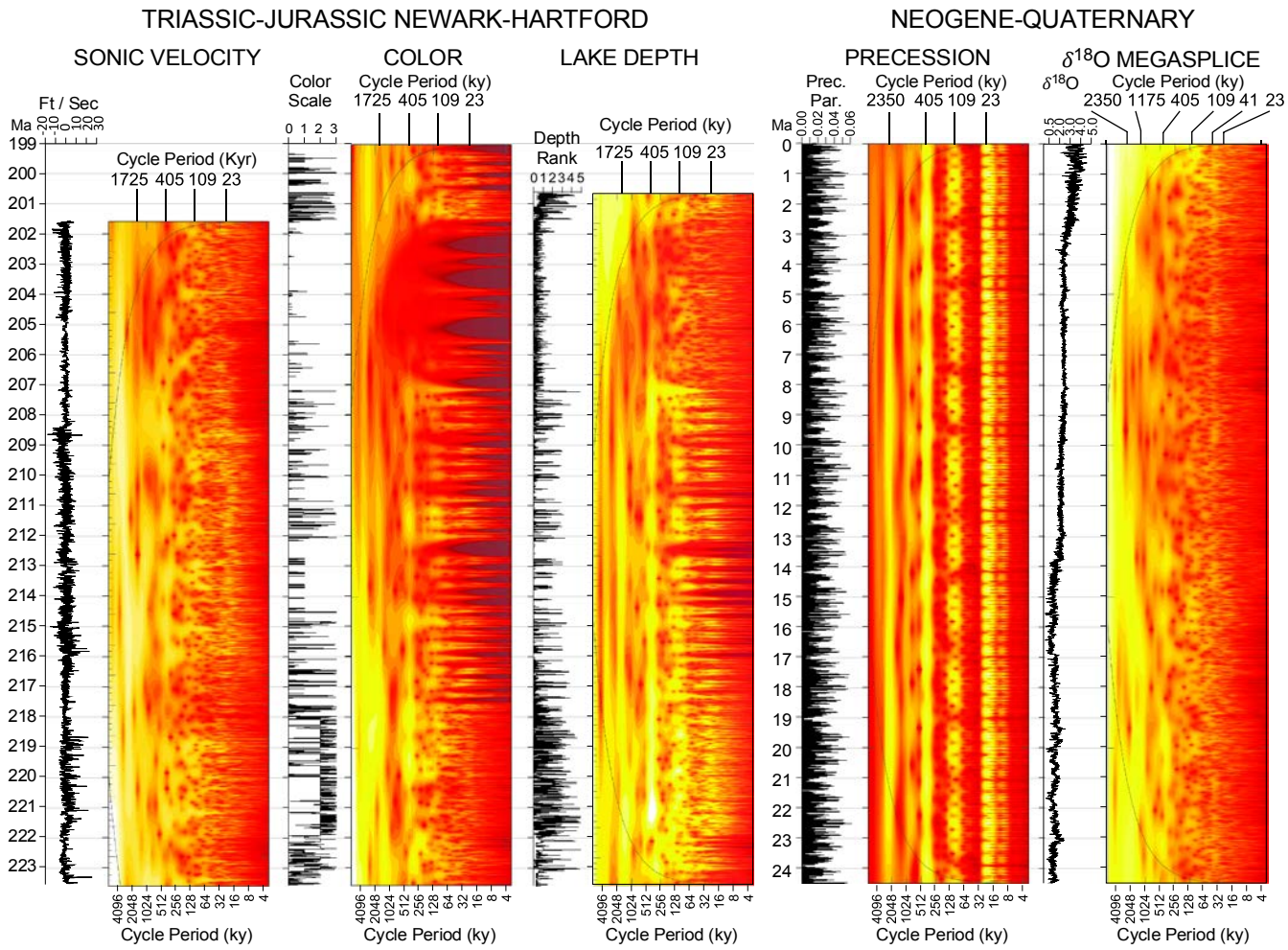
TRIASSIC-JURASSIC NEWARK-HARTFORD
NEOGENE-QUATERNARY
SONIC VELOCITY
COLOR
LAKE DEPTH
PRECESSION
δ18O MEGASPLICE
Ft / Sec
Ma
Cycle Period (Kyr)
1725 405 109 23
Color Scale
Cycle Period (ky)
Depth Rank
Prec. Par.
2350 405 109 23
δ18O
2350 1175 405 109 41 23
4096 2048 1024 512 256 128 64 32 16 8 4

Figure 6

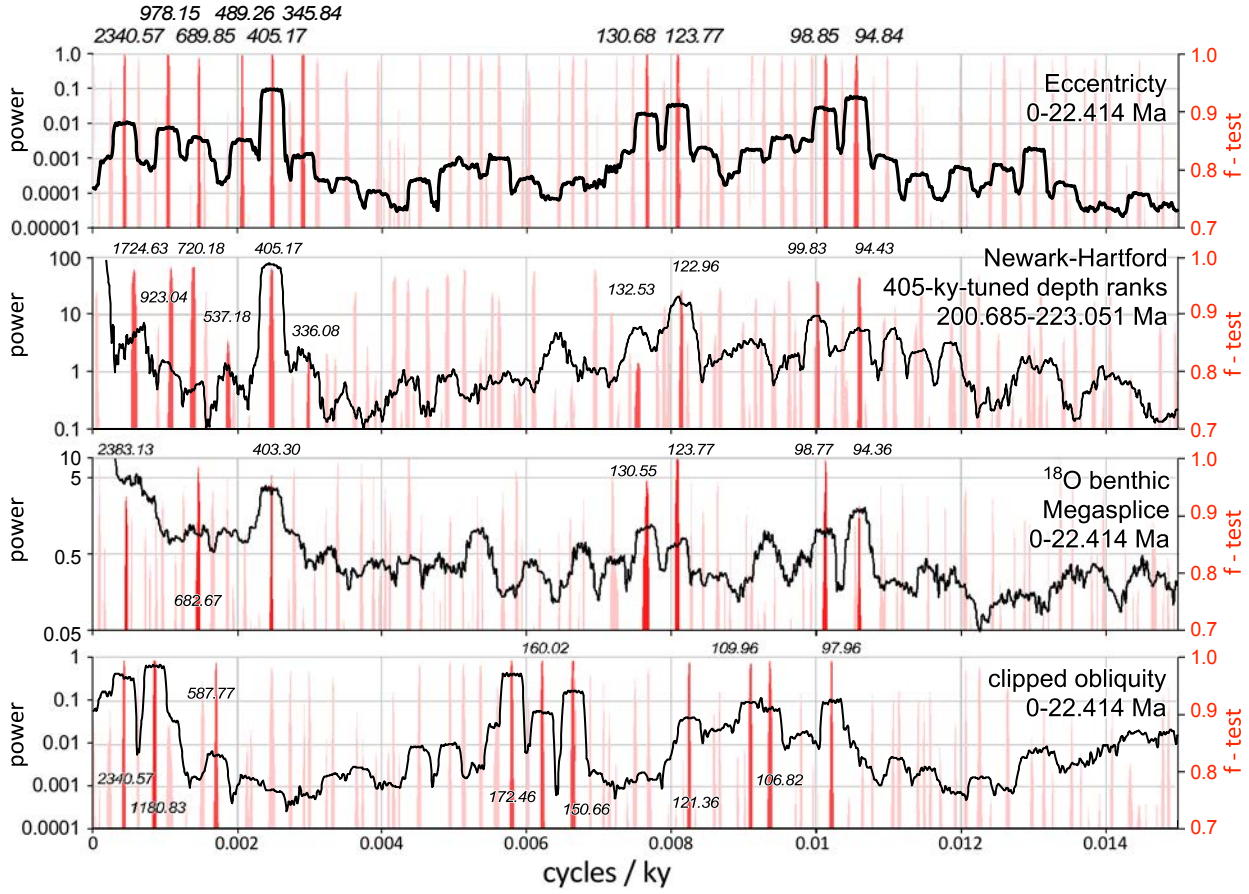
978.15 489.26 345.84
2340.57 689.85 405.17
130.68 123.77
98.85 94.84
Eccentricty
0-22.414 Ma
power
f - test
1724.63 720.18 405.17
99.83 94.43
923.04
537.18
336.08
132.53
122.96
Newark-Hartford
405-ky-tuned depth ranks
200.685-223.051 Ma
2383.13
403.30
123.77
98.77 94.36
130.55
682.67
18O benthic
Megasplice
0-22.414 Ma
160.02
109.96
97.96
587.77
2340.57
1180.83
172.46
150.66
121.36
106.82
clipped obliquity
0-22.414 Ma
0 0.002 0.004 0.006 0.008 0.01 0.012 0.014
cycles / ky

Figure 7

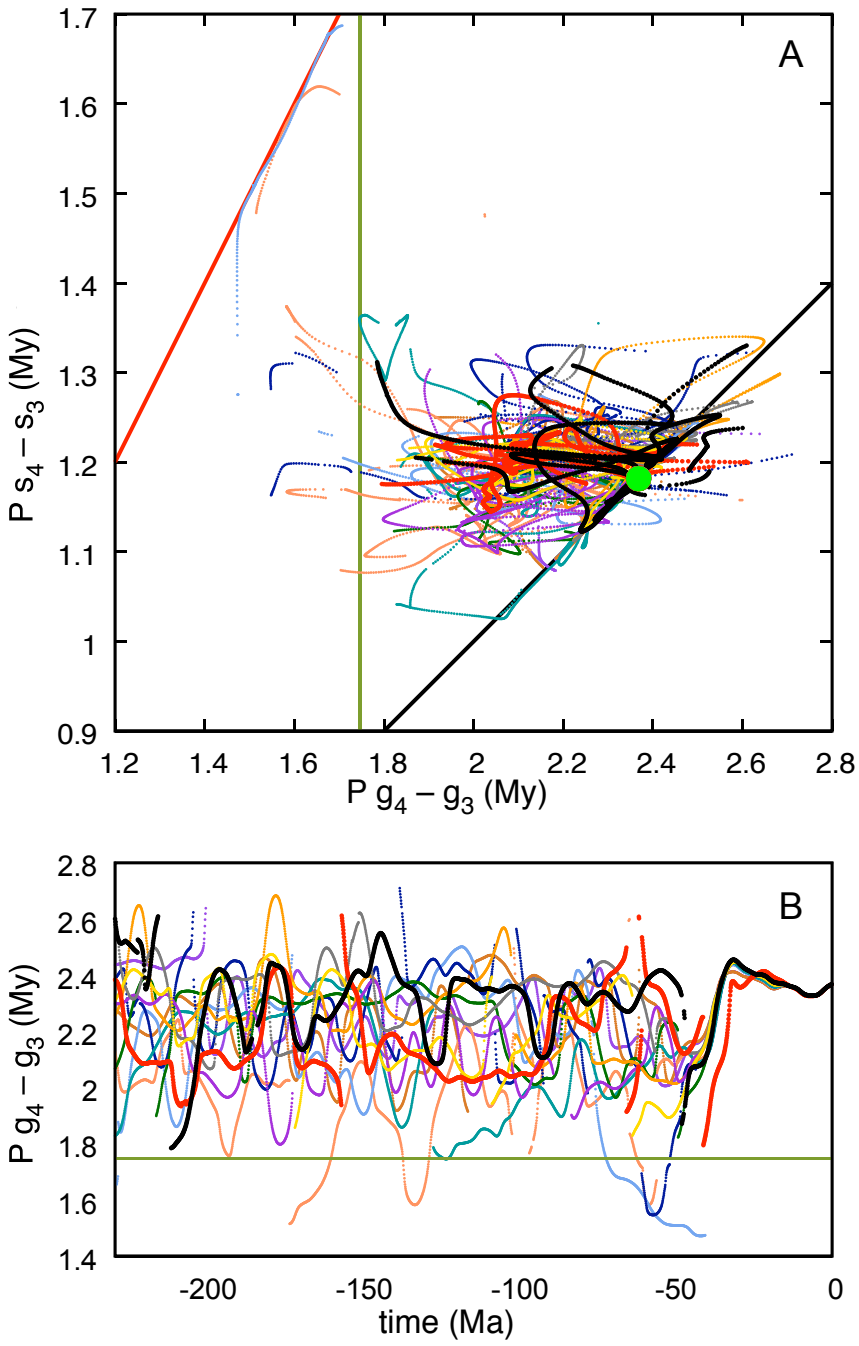
A
B
P $s_4 - s_3$ (My)
P $g_4 - g_3$ (My)
P $g_4 - g_3$ (My)
time (Ma)
1.7
1.6
1.5
1.4
1.3
1.2
1.1
1
0.9
1.2
1.4
1.6
1.8
2
2.2
2.4
2.6
2.8
-200
-150
-100
-50
0

Table 1: : Cycle Nomenclature and Origins

Lithological Expression of Cycles*	**Description**	**Argument**	**Periods and Informal Names of Milankovitch or Orbital Cycle with Today's Period****	
Van Houten Cycle	Precession frequency of Earth (p) + secular frequency of precession of perihelion of Mercury (g_1) …	$p + g_1$, $p + g_2$, $p + g_3$, $p + g_4$, $p + g_5$	~21 ky (Average 21.5 ky) 23.2, 22.4, 19.2, 19.0, 23.8 ky Climatic Precession	
Short Modulating Cycle	Secular frequency of precession of perihelion of Mars (g_4) – that of Jupiter (g_5) …	$g_4 - g_5$, $g_3 - g_2$, $g_4 - g_2$, $g_3 - g_2$	~100 ky (Average 112.1 ky) 94.9, 98.9, 123.9, 130.7 ky Short Orbital Eccentricity cycles	
McLaughlin Cycle	Venus (g_2) – Jupiter (g_5)	g_2-g_5	405 ky Long Orbital Eccentricity	Grand Cycles
None	Venus (g_2) –Mercury (g_1)	g_2-g_1	696 ky none	
None	Mercury (g_1) – Jupiter (g_5)	g_1-g_5	973 ky none	
Long Modulating Cycle	Mars (g_4) – Earth (g_3)	g_4-g_3	2365 ky none	

*From ref. 9.

**Using the g_1, g_2, g_3, g_4, g_5 values from ref. 34, Table 6 and p from ref. 31, Table 1.

Table 2: Periods in Newark-Hartford Data

	Argument (frequency)	MTM period (ky)	FA period (ky)	La2010d* period (ky)	La2010a period (ky)
1	g_4-g_3	1724.63	1747.65	1793.04	2368.95
2	g_1-g_5	923.04	923.16	957.56	967.42
3	g_2-g_1	720.18	719.05	704.98	697.63
4	(g_2-g_5)-(g_4-g_3)	537.18	527.56	515.09	489.37
5	g_2-g_5	405.17	404.97	404.58	405.63
6	(g_2-g_5)+(g_4-g_3)	336.53	335.13	330.08	346.42
7	g_3-g_2	132.53	132.17	132.58	130.71
8	g_4-g_2	122.96	123.08	123.47	123.88
9	g_3-g_5	99.83	99.78	99.86	98.85
10	g_4-g_5	94.43	94.49	94.62	94.89

Table 3: Secular Fundamental Frequencies and Consistency Relations

	Argument	MTM (“/yr)	FA (“/yr)	FA-La2010d* residual (“/yr)	La2010d* (“/yr)	La2010 (“/yr)
0	g_5	4.257482	4.257482		4.257438	4.257482
1	g_4-g_3	0.742	0.727	0.014		
2	g_1	5.662	5.661	0.050	5.611	5.59
3	g_2-g_1	1.795	1.796	0.006		
4	(g_2-g_5)-(g_4-g_3)	2.456	2.473	-0.016		
5	g_2	7.456	7.458	-0.003	7.461	7.453
6	g_3-g_2	9.783	9.788	0.017		
7	g_4-g_2	10.526	10.516	0.014		
8	g_3	17.240	17.246	0.010	17.236	17.368
9	g_4	17.982	17.973	0.018	17.955	17.916